


The anti-human cytomegalovirus drug triclin inhibits cyclin-dependent kinase 9

Hidetaka Sadanari¹, Kazuhiro J. Fujimoto¹ , Yuto Sugihara¹, Tomoki Ishida¹, Masaya Takemoto¹, Tohru Daikoku² and Tsugiyu Murayama²

¹ Center for Basic Education, Faculty of Pharmaceutical Sciences, Hokuriku University, Kanazawa, Japan

² Department of Microbiology and Immunology, Faculty of Pharmaceutical Sciences, Hokuriku University, Kanazawa, Japan

Keywords

anti-cytomegalovirus agent; cyclin-dependent kinase 9; cytomegalovirus replication; triclin

Correspondence

K. J. Fujimoto, Center for Basic Education, Faculty of Pharmaceutical Sciences, Hokuriku University, Ho-3 Kanagawa-machi, Kanazawa 920-1181, Japan
Fax: +81-76-229-2781
Tel: +81-76-229-6191
E-mail: k-fujimoto@hokuriku-u.ac.jp
and

T. Murayama, Department of Microbiology and Immunology, Faculty of Pharmaceutical Sciences, Hokuriku University, Ho-3 Kanagawa-machi, Kanazawa 920-1181, Japan
Fax: +81-76-229-2781
Tel: +81-76-229-2346
E-mail: t-murayama@hokuriku-u.ac.jp

(Received 29 November 2017, revised 26 January 2018, accepted 30 January 2018)

doi:10.1002/2211-5463.12398

4',5,7-trihydroxy-3',5'-dimethoxyflavone (triclin), derived from *Sasa albo-marginata*, has been reported to suppress significantly human cytomegalovirus (HCMV) replication in human embryonic lung (HEL) fibroblast cells. However, the target protein of triclin remains unclear. This study focused on the anti-HCMV activity of triclin in terms of its binding affinity to cyclin-dependent kinase 9 (CDK9). A molecular docking study predicted that triclin binds well to the ATP-binding site of CDK9. Experimental measurements then revealed that triclin inhibits the kinase activity of CDK9 and affects the phosphorylation of the carboxy-terminal domain of RNA polymerase II. Based on these results, we conclude that CDK9 is one of the target proteins of triclin. We also found that triclin possesses anti-HCMV activity with no cytotoxicity against HEL cells.

Human cytomegalovirus (HCMV), also known as human herpesvirus 5, is a widespread viral pathogen that causes serious diseases in newborn infants and immunocompromised patients [1–4]. Highly potent drugs such as ganciclovir, valganciclovir, foscarnet, and cidofovir are now available for HCMV treatment. These compounds inhibit viral DNA synthesis by

targeting the HCMV DNA polymerase (Enzyme Commission number: EC 2.7.7.7) [5]. However, prolonged administration of anti-HCMV agents induces antiviral drug resistance, leading to a recurrent problem in the treatment of immunocompromised patients. In addition, anti-HCMV agents cause frequent adverse side effects such as bone marrow suppression [6,7] and

Abbreviations

CC₅₀, 50% cytotoxic concentration; CDK9, cyclin-dependent kinase 9; CTD, carboxy-terminal domain; CycK, cyclin K; CycT1, cyclin T1; EC₅₀, 50% effective concentration; F/ABCps, fitness learning-based artificial bee colony with proximity stimuli; HCMV, human cytomegalovirus; HEL, human embryonic lung; hpi, hours postinfection; IC₅₀, 50% inhibitory concentration; IE, immediate early; LDH, lactate dehydrogenase; RMSD, root-mean-square deviation; Ser2-P, serine 2 phosphorylation; Ser5-P, serine 5 phosphorylation; SI, selective index.

nephrotoxicity [6,8,9] because of their toxicities. To circumvent these problems, a novel type of anti-HCMV drug is required.

4',5,7-trihydroxy-3',5'-dimethoxyflavone (triclin; Fig. 1A), derived from *S. albo-marginata*, has been shown to suppress significantly the replication of HCMV and influenza virus [10–12]. Moreover, the compound has been shown to inhibit viral gene expression of immediate early (IE) 2 and UL54 (DNA polymerase) in a dose-dependent manner [10]. Furthermore, the action of triclin was found to affect the expression of chemokines [13,14]. These results indicate that triclin does not bind to HCMV DNA polymerase. However, the target protein of triclin remains unclear.

Cyclin-dependent kinases (CDKs; EC 2.7.11.22) are known to be involved in viral replication [15–18]. It has been reported that cyclin-dependent kinase 9 (CDK9)/cyclin T1 (CycT1) in mammalian cells initiates transcriptional elongation of genes by phosphorylating one serine residue, serine 2 (Ser2), within the carboxy-terminal domain (CTD) of RNA polymerase II (RNA pol II) [19]. In addition, CDK9 contributes to the phosphorylation of Ser5 near transcription start sites [20]. Such phosphorylation activities of CDKs are inhibited by a synthetic flavonoid, flavopiridol (Fig. 1B) [21–23]. X-ray crystallographic analysis has revealed that flavopiridol binds to the ATP-binding site of CDK9 [24]. As triclin is structurally similar to

flavopiridol, these findings raise the possibility that triclin directly inhibits CDK9, thereby inhibiting viral RNA transcription.

In this study, we investigated whether triclin binds to CDK9 and suppresses viral RNA transcription. For this purpose, we first performed molecular docking simulations using a novel optimization algorithm called fitness learning-based artificial bee colony with proximity stimuli (F/ABCps) [25–28]. The docking simulation successfully provided the binding conformation of triclin in the binding site of CDK9. Subsequently, we evaluated the *in vitro* kinase inhibitory activity of triclin against CDK9 and tested whether triclin affects *in vivo* the phosphorylation of CTD of RNA pol II. We also evaluated the cellular antiviral potency of triclin and its cytotoxicity, which were compared with those of flavopiridol.

Materials and methods

Molecular docking study

The structures of triclin and flavopiridol shown in Fig. 1A and B, respectively, were optimized with density-functional theory at the B3LYP/6-31G* level [29]. Atomic charges of the ligands were derived from electrostatic potential fitting [30]. All electronic structure calculations were performed with the Gaussian 09 program package [31]. Atomic

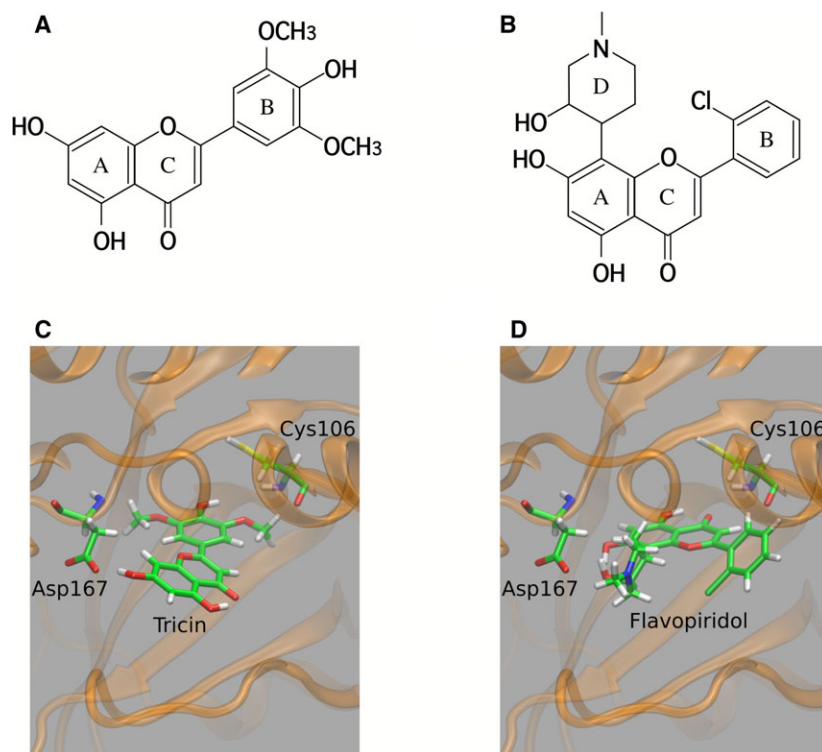


Fig. 1. Chemical structures of (A) triclin and (B) flavopiridol. Docking poses of (C) triclin and (D) flavopiridol in the binding site of CDK9. In (A) and (B), the definitions of the rings, that is, A–C for triclin and A–D for flavopiridol, are also shown. In (C) and (D), the brown ribbon represents the backbone structure of CDK9. In (C), the OH groups in the A- and B-ring of triclin are directed toward Asp167 and Cys106, respectively. In (D), the D-ring of flavopiridol is located close to Asp167, and the carbonyl oxygen of the C-ring is directed toward Cys106.

coordinates of human CDK9 were taken from the crystal structure (PDB ID: 3BLR [24]). This crystal structure also contained flavopiridol. The molecular docking simulations with F/ABCps [27] were carried out for a cubic box ($22.5 \times 22.5 \times 22.5 \text{ \AA}^3$) at the ATP-binding site of CDK9, in which the AutoDock force field [32] was employed to calculate the scoring function. The maximum number of energy evaluations before the termination of F/ABCps was set to 2 500 000.

Cell and virus

Human embryonic lung (HEL) fibroblast cells [33] were grown in Dulbecco's modified Eagle's medium (Nissui Pharmaceutical Inc., Tokyo, Japan) as described previously [10]. HCMV strain Towne was used in all experiments. The history of this strain has been described elsewhere [34,35]. HCMV was propagated in HEL cells. Infectious virus production was titrated using a plaque assay as described previously [35].

Compounds

Tricin was synthesized as described previously [10,11], and flavopiridol was purchased from Cayman Chemical (Ann Arbor, MI, USA). Both compounds were dissolved at indicated concentrations as a stock solution in DMSO and stored at $-80 \text{ }^\circ\text{C}$ until use. The final concentration of DMSO in cell culture was adjusted 0.1%.

In vitro enzymatic kinase assay for CDK9

As CDK9 activation requires binding of CycT or cyclin K (CycK), we used a CDK9/CycK kinase assay in this study. Kinase activity and inhibition were measured by quantifying the amount of ADP converted from ATP during a kinase reaction by the ADP-Glo™ kinase assay (Promega Japan Inc., Tokyo, Japan). Kinase reactions were performed in kinase reaction buffer [40 mM Tris (pH 7.5), 20 mM MgCl_2 , 0.1 $\text{mg}\cdot\text{mL}^{-1}$ BSA, and 50 μM dithiothreitol] supplemented with 10 μM ATP, CDK9/CycK kinase, and PDKtide synthetic peptide as substrates, according to the manufacturer's protocol. Briefly, kinase reactions were started by adding 2 μL of the ATP/substrate (final concentration of 0.2 $\mu\text{g}\cdot\mu\text{L}^{-1}$ PDKtide) to mixtures of 1 μL of 5 \times concentrated drug (diluted in final concentrations of 5% DMSO) and 2 μL of kinase solution (containing 30 ng CDK9/CycK), incubated for 2 h at room temperature (22–25 $^\circ\text{C}$), and then stopped by adding 5 μL of ADP-Glo reagent. After incubation of the reaction mixture at room temperature for 40 min, 10 μL of kinase detection reagent was added, and then the mixture was incubated for an additional 40 min. Subsequently, the luminescence intensity was measured by a luminometer (MiniLumat LB 9506, Berthold Technologies, Bad

Wildbad, Germany). This assay is sensitive enough to detect very low amounts of ADP (20 nM) in a linear fashion. No-enzyme and no-inhibitor reactions represented background luminescence (0% activity) and noninhibited kinase activity (100% activity), respectively. The percent kinase activity was calculated by (a) subtracting the averaged value of no-enzyme reaction luminescence from that of the kinase-containing reaction with or without inhibitor and (b) converting these net luminescence values to percent activity based on no-inhibitor reactions, which represented 100% kinase activity.

Western blot analysis

Western blot analysis was performed as described previously [11]. Briefly, cells were lysed in SDS sample buffer [62.5 mM Tris/HCl (pH 6.8), 2% SDS, 10% glycerol, 5% 2-mercaptoethanol] and cell lysates were subjected to electrophoresis on 5–15% SDS/PAGE (Bullet PAGE One Precast gel; Nacalai Tesque Inc., Kyoto, Japan) and transferred to polyvinylidene difluoride membranes (GE Healthcare, Little Chalfont, UK (formerly Amersham Bioscience, Little Chalfont, UK)). The blots were blocked in TBS-T [20 mM Tris/HCl (pH 7.5), 150 mM NaCl, 0.1% Tween 20] with 5% skim milk for 1 h and reacted with primary antibody diluted in TBS-T plus 5% skim milk overnight at 4 $^\circ\text{C}$. After washing with TBS-T, the blots were incubated with horseradish peroxidase-conjugated anti-IgG (Cell Signaling Technology Japan Inc., Tokyo, Japan) in TBS-T plus 5% skim milk for 1 h, washed in TBS-T, and then developed by enhanced chemiluminescence according to the manufacturer's protocol (GE Healthcare). For a loading control, after detection of the protein of interest, the membrane was stripped and re probed with anti- β -actin antibody conjugated with horseradish peroxidase (Abcam, Cambridge, UK) according to the Amersham ECL protocol. Anti-phospho-Ser2 RNA pol II and anti-phospho-Ser5 RNA pol II antibodies, which specifically recognize the Ser2- and Ser5-phosphorylated forms within the CTD of RNA pol II, respectively, were purchased from Bethyl Laboratories (Montgomery, TX, USA).

Plaque reduction assay

HEL cells were grown in 24-well plates to more than 90% confluence and infected with HCMV at around 100 PFU per well. Following 90-min adsorption, the medium was aspirated from the wells, and fresh medium containing selected drug dilutions of triclin and flavopiridol and 0.4% of agarose was added into triplicate wells. After incubation at 37 $^\circ\text{C}$ for 6–8 days, the cell monolayer was fixed with 10% formalin and then stained with 0.05% crystal violet. Plaques were counted microscopically under low power. Drug effects were calculated as the percent reduction in the number of plaques in the presence of each drug concentration to the number of plaques observed in the absence of drug.

Cell toxicity assays

To measure cytotoxic effects of triclin and flavopiridol, the CytoTox 96 assay kit (Promega Japan Inc.) was used according to the manufacturer's instructions. The CytoTox 96 assay kit quantitatively measures a cytosolic enzyme, lactate dehydrogenase (LDH), which is released upon cell lysis. A total of 10 000 cells were plated in a 96-well tissue culture plate in triplicate, and serum-free medium containing various concentrations of the drug was present before the cytotoxicity assays. The released LDH is able to convert the substrate tetrazolium salt into a red formazan product, which can be measured at 492 nm in a 96-well tissue culture plate. To determine the percent cytotoxicity, the amount of LDH released by cells after drug treatment was compared and normalized with the amount of LDH released after complete cell lysis.

Results

Triclin is predicted to strongly bind to CDK9

We first performed redocking calculations 1000 times with the crystal structure of CDK9 and flavopiridol (PDB ID: 3BLR). As a result, the lowest energy pose of flavopiridol successfully reproduced the crystal structure with a root-mean-square deviation (RMSD) of 0.53 Å. The docking poses with the RMSD < 1.0 Å were obtained 848 times out of 1000 runs. These results showed that the F/ABCps method is applicable to this system.

We next investigated whether triclin binds to CDK9. Molecular docking simulations with F/ABCps were performed 1000 times. Figure 1C shows the docking pose of triclin with the lowest energy in the binding site of CDK9. The A-ring of the flavone skeleton is located close to Asp167, and the OH-group in the B-ring is directed toward Cys106. The docking poses of triclin with an RMSD < 1.0 Å from the lowest energy pose were obtained 485 times out of 1000 runs. Table 1 summarizes the predicted binding energies of the best scoring poses. The binding energy between triclin and CDK9 was calculated to be -5.77 kcal·mol⁻¹. We also took the average of the 1000 binding energies, which yielded a result of -5.56 kcal·mol⁻¹. From these results, triclin was predicted to bind well to CDK9.

The results of flavopiridol were also compared with those of triclin. Figure 1D illustrates the lowest energy pose of flavopiridol obtained with F/ABCps. As shown, the direction of flavopiridol is different from that of triclin. The D-ring of flavopiridol is located close to Asp167, while the carbonyl oxygen of the C-ring is directed toward Cys106. The binding energy of

Table 1. CDK9-ligand binding energies (kcal·mol⁻¹).

	Lowest value ^a	Mean value ^b
Triclin	-5.77	-5.56
Flavopiridol	-6.65	-6.56

^aThe lowest value of the 1000 runs.

^bMean value calculated with the 1000 binding energies.

the best scoring pose and the mean value were calculated to be -6.65 and -6.56 kcal·mol⁻¹, respectively. These results showed lower binding energies for flavopiridol than for triclin. Thus, flavopiridol was predicted to bind to CDK9 stronger than triclin.

Triclin inhibits the kinase activity of the CDK9/CycK complex

Based on the computational results, we experimentally investigated the kinase inhibitory activity of triclin against CDK9. As shown in Fig. 2A, triclin inhibited the kinase activity of the CDK9/CycK complex in a dose-dependent manner. Although the kinase activity at more than 10 μM triclin could not be assessed due to triclin precipitation, the 50% inhibitory concentration (IC₅₀) of triclin was evaluated to be 1.38 ± 0.83 μM, which resulted in a higher value than those of other CDK9 inhibitors [36,37]. As mentioned above, flavopiridol is a widely known CDK inhibitor [21]; thus, we also measured the kinase inhibitory activity of flavopiridol for comparison. As shown in Fig. 2B, the kinase activity of the CDK9/CycK complex was dramatically inhibited by flavopiridol. The IC₅₀ of flavopiridol was calculated to be 8.20 ± 2.54 nM, similar to previously published values (4.59 nM [38] and 11 nM [39]). From these results, we confirmed that triclin inhibits the kinase activity of CDK9 and that its inhibitory activity is weaker than that of flavopiridol, which correlates with the results of the docking simulations.

Triclin inhibits the phosphorylation of Ser2 and Ser5 within the CTD of RNA pol II

We next investigated the effect of CDK9 inhibition by triclin on *in vitro* cell culture of HEL cells. One established cellular target of CDK9 is Ser2 and Ser5 within the CTD of RNA pol II. The inhibition of phosphorylation at these two sites has been reported to suppress the transcription of IE genes of HCMV [15]. As shown in Fig. 3A, in HCMV-infected HEL cells, the levels of Ser2 and Ser5 phosphorylation (Ser2-P and Ser5-P, respectively) remained relatively constant between 1

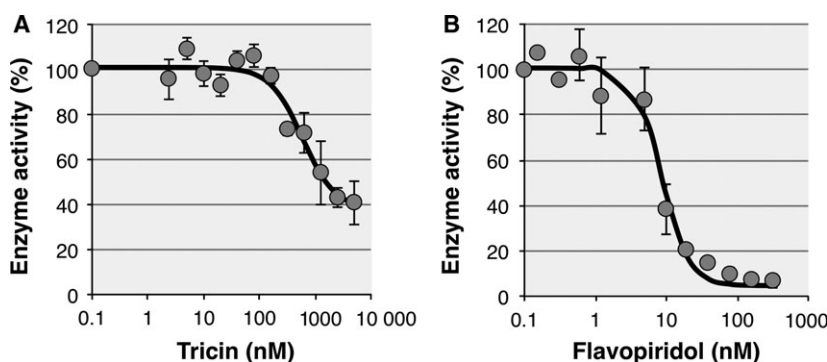


Fig. 2. Effect of triclin on the kinase activity of the CDK9/CycK complex. Kinase assays were performed and quantitated as described in the Materials and methods. The lanes (left to right) are from reactions containing 2.44–5000 nM triclin (A) or 0.152–312.5 nM flavopiridol (B), both of which were prepared by making twofold serial dilutions. The percent kinase activity was calculated as described in the Materials and methods. The IC_{50} values were calculated by fitting the data to a logistic dose–response curve using curve-fitting tools in NIH IMAGEJ software (National Institute of Health, Bethesda, MD, USA). Each inhibition curve was performed more than twice on different experiments.

and 5 h postinfection (hpi). However, these levels dramatically increased to maxima until 48 hpi and remained at maxima at 72 hpi (Fig. 3A, upper and middle panels, lanes 1–8). Figure 3B shows the relative densitometric analyses of the blots, normalized to β -actin levels. In uninfected HEL cells (Fig. 3B, white bars), the relative levels of Ser2-P and Ser5-P at 48 and 72 hpi were augmented 1.8-fold or more than those at 0 hpi. In contrast, the levels of Ser2-P and Ser5-P gradually decreased until 5 hpi in HCMV-infected cells treated with 10 μ M triclin, then increased between 8 and 72 hpi (Fig. 3A, upper and middle panels, lanes 9–16). This time course study clearly demonstrated triclin treatment significantly reduces the relative levels of both Ser2-P and Ser5-P (Fig. 3B).

Next, the same analysis was performed with flavopiridol. As also shown in Fig. 3A, the levels of Ser2-P and Ser5-P quickly decreased at 1 hpi in HCMV-infected cells treated with 62.5 nM flavopiridol. These levels remained relatively stable up to 8 hpi, and then gradually increased (Fig. 3A, upper and middle panels, lanes 19–24). Consequently, the temporal profile (time course) for flavopiridol treatment was almost the same as that for triclin treatment (Fig. 3B, black bars vs. gray bars).

We also performed the same measurements with mock-infected HEL cells treated with triclin. As shown in Fig. 3C, the levels of Ser2-P and Ser5-P decreased slightly but significantly between 1- and 5-h treatment and increased gradually until 72-h treatment. The relative levels of Ser2-P and Ser5-P at 72-h treatment increased to 1.1- and 1.4-fold of those in untreated cells, respectively (Fig. 3D).

These results indicate that triclin inhibits the phosphorylation at Ser2 and Ser5 within the CTD of RNA

pol II for up to 8 hpi and this inhibition continues until at least 72 hpi. As shown by black and gray bars in Fig. 3B, the inhibition levels of triclin on the phosphorylation seem to be weaker than those of flavopiridol. However, the temporal profile (time course) of the inhibition by triclin is found to be similar to that by flavopiridol (Fig. 3B). These results strongly suggest that the inhibition of phosphorylation at Ser2 and Ser5 by triclin is attributed to its inhibition of the CDK9 kinase activity, as reported for flavopiridol [23].

Comparison of anti-HCMV activity between triclin and flavopiridol

To further investigate the anti-HCMV effects of triclin and flavopiridol, the plaque reduction assay was performed. As shown by the black line in Fig. 4A, triclin had anti-HCMV activity with a 50% effective concentration (EC_{50}) of $2.09 \pm 0.50 \mu$ M, which showed a similar value to the CDK9 kinase inhibitory activity ($1.38 \pm 0.83 \mu$ M). Conversely, the EC_{50} of flavopiridol was 15.8 ± 3.2 nM (Fig. 4B). This value was also similar to the CDK9 kinase inhibitory activity of flavopiridol (8.20 ± 2.54 nM). These results strongly suggest that the anti-HCMV effects of triclin are also caused by the inhibition of the CDK9 kinase activity.

Although flavopiridol is well known as a potent CDK inhibitor [21], it is considered to be highly cytotoxic [22]. For this reason, we next investigated the cytotoxic effect of triclin and flavopiridol in HEL cells. As shown by the gray line in Fig. 4A, triclin had no cytotoxic effect at all concentrations tested in this experiment. Conversely, flavopiridol was cytotoxic at concentrations approximately 10-fold higher than the EC_{50} value obtained by the plaque reduction assay (Fig. 4B, gray line).

Fig. 3. Effect of tricrin on the levels of Ser2-P and Ser5-P in HEL cells. (A) HEL cells cultured to semiconfluence (more than 80%) were infected with HCMV at an MOI of 1 PFU per cell in the absence or presence of 10 μ M tricrin or 62.5 nM flavopiridol. At the indicated time points, cells were harvested in lysis buffer and the concentrations of Ser2-P or Ser5-P were determined by western blot analysis. (C) HEL cells cultured to semiconfluence (more than 80%) were treated with 10 μ M tricrin, and cells were harvested in lysis buffer at the indicated time points. (B and D) Band intensities were quantitated using NIH IMAGEJ software, and the levels were normalized to those of β -actin (internal control). The results shown are the mean and SD of three different experiments. *P* values were calculated using Student's *t*-test. **P* < 0.05, HCMV-infected or HCMV-infected and flavopiridol-treated cells compared with HCMV-infected and tricrin-treated cells (B); **P* < 0.05, tricrin-treated cells compared with uninfected and untreated cells (D).

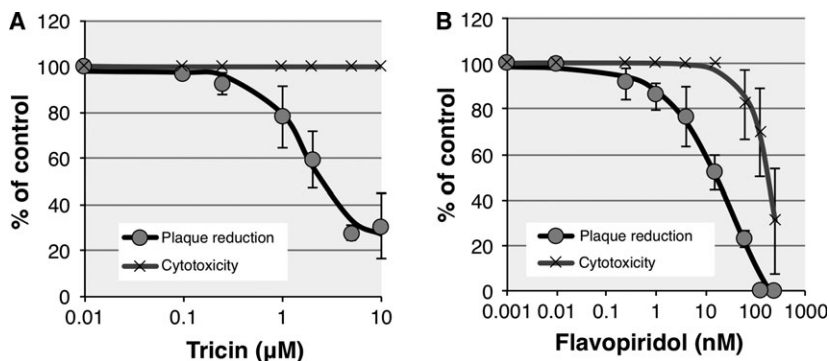
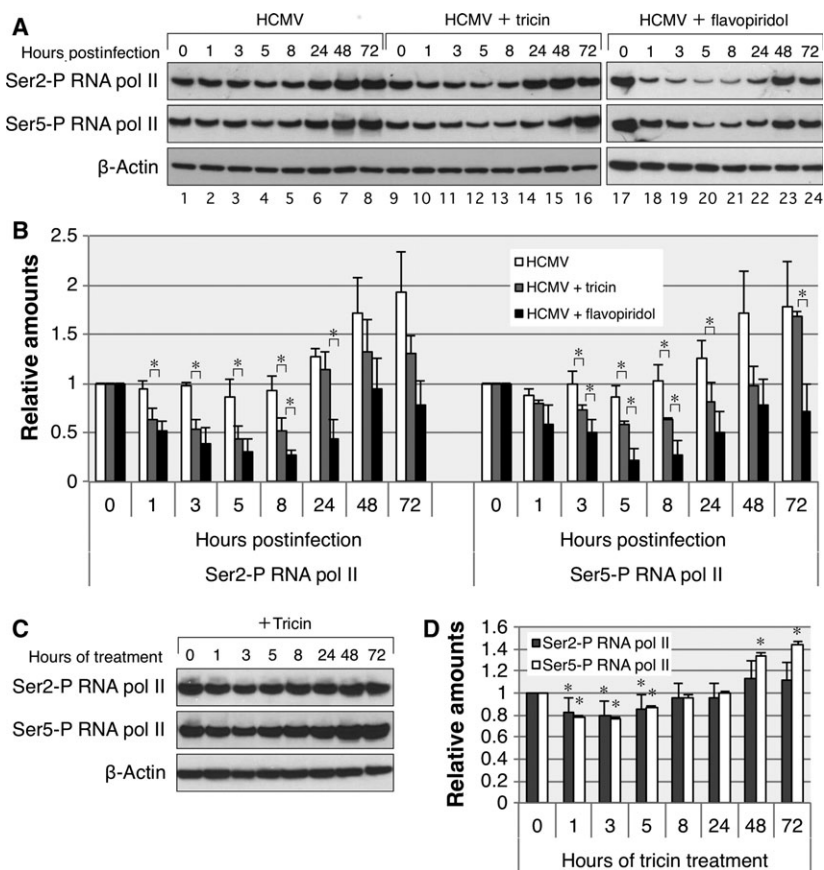


Fig. 4. Comparison of anti-HCMV activity and cytotoxicity between flavopiridol and tricrin. HEL cells (1.5×10^5 cells) plated in 24-well plates were infected with HCMV and treated with various concentrations of flavopiridol or tricrin during and after infection for 7 days. The antiviral activity was then determined in a PFU reduction assay. Cytotoxicity of the two compounds was determined by incubating HEL cells in 96-well plates with various concentrations of flavopiridol or tricrin for 7 days in triplicate, followed by measurement of LDH release as described in the Materials and methods.

Evaluation with the LDH leakage assay provided a 50% cytotoxic concentration (CC_{50}) of 176 ± 29 nM for flavopiridol. Taking into account the EC_{50} value of flavopiridol (15.8 ± 3.2 nM), the selective index ($SI = CC_{50}/EC_{50}$) of flavopiridol was calculated to be 11.1, indicating low to moderate potential as an

antiviral agent. From these results, we could confirm that flavopiridol possesses not only strong anti-HCMV activity but also strong cytotoxicity. In contrast, no cytotoxic effect was observed for tricrin in the present experiment; thus, tricrin is considered the preferred candidate for anti-HCMV drug development.

Discussion

In this study, we investigated the anti-HCMV effect of triclin in terms of its binding affinity to CDK9. Molecular docking study with the F/ABCps method predicted that triclin binds well to the binding site of CDK9. As X-ray crystallographic analysis was not performed in this study, we cannot compare the predicted pose of triclin with the crystal structure. However, the predicted structure of triclin is considered to be reliable because F/ABCps successfully reproduced the correct binding pose of flavopiridol with an RMSD of 0.53 Å from the crystal structure. It should be noted that redocking with crystal structure is not a trivial problem for molecular docking study [40]. A docking pose with an RMSD of < 2 Å is commonly regarded to indicate successful reproduction of the crystal ligand. We also calculated the binding energy of the crystallographic position of flavopiridol, which yielded a result of $-6.13 \text{ kcal}\cdot\text{mol}^{-1}$. This value was larger by $0.52 \text{ kcal}\cdot\text{mol}^{-1}$ than the lowest binding energy obtained with F/ABCps ($-6.65 \text{ kcal}\cdot\text{mol}^{-1}$). As mentioned above, the lowest energy pose of flavopiridol was almost the same as the crystal structure (RMSD = 0.53 Å); thus, these results may indicate that a slight difference in the ligand structure (e.g., positions of hydrogen atoms) strongly influences the interactions between CDK9 and flavopiridol. Molecular docking study also predicted that the binding affinity for triclin to CDK9 is weaker than that of flavopiridol to CDK9. Despite their similar structures, the binding poses of triclin and flavopiridol showed different directions, which resulted in different binding energy values.

The computational predictions were next verified experimentally by measuring the kinase inhibitory activity of triclin against CDK9, where flavopiridol was also evaluated for comparison. As predicted by the docking simulations, the experimental results clearly demonstrated that triclin inhibits the CDK9 kinase activity, while the IC_{50} value of triclin was approximately 170-fold higher than that of flavopiridol. Subsequently, we investigated the influence of triclin on the phosphorylation at Ser2 and Ser5 within the CTD of RNA pol II. The experimental analysis revealed that triclin inhibits the phosphorylation of both Ser2 and Ser5, and its time course profile is similar to that of flavopiridol. Flavopiridol is known to reduce the phosphorylation activity of CDK9 at Ser2 and Ser5 within the CTD of RNA pol II. Therefore, the present results strongly suggested that the reduction in the phosphorylation at Ser2 and Ser5 by triclin is attributed to the inhibition of the CDK9 kinase activity.

We also evaluated the cellular anti-HCMV potencies of triclin and flavopiridol. Triclin was shown to have

anti-HCMV activity, although its potency was weaker than that of flavopiridol. Moreover, the EC_{50} value of triclin on the anti-HCMV activity was shown to be comparable to the IC_{50} value on the CDK9 kinase inhibitory activity. These results could be interpreted that the anti-HCMV effects of triclin are caused by the inhibition of the CDK9 kinase activity. Based on these results, we concluded that CDK9 is one of the target proteins of triclin.

We finally measured the cytotoxicity of triclin and flavopiridol. Flavopiridol demonstrated strong cytotoxicity against HEL cells, while no cytotoxic effect was observed for triclin. Furthermore, the SI value of flavopiridol was estimated to be 11.1, which indicated that flavopiridol has low to moderate potential as an antiviral agent. Conversely, Sakai *et al.* [41] reported that the SI value of triclin was 1206. Taken together, these results suggest that triclin is the preferred candidate for anti-HCMV drug development.

In this study, we focused on the CDK9 kinase inhibitory activity of triclin and concluded that CDK9 is one of the target proteins of triclin. On the other hand, we have also revealed that the action of triclin affects the expression of chemokines [13,14]. These results strongly suggest that the inhibition of HCMV replication by triclin cannot be explained by its effect on CDK9 alone. It is necessary to address whether the activity of other CDKs is inhibited by triclin and consequently which steps of HCMV replication are disrupted. Such studies will be performed in our future work.

Acknowledgements

This study was supported by JSPS KAKENHI Grant (Nos. 15K09587, 24591492, and 16K05670), the 30th Hokkoku Foundation for Cancer Research, and the Specific Research Fund of Hokuriku University (2015–2016).

Author contributions

KJF and TM conceived and supervised the study; HS and TM designed experiments; KJF performed simulation studies; HS, YS, and TI performed experiments; HS, MT, and TD analyzed data; KJF and HS wrote the manuscript; TM, MT, and TD made manuscript revisions.

References

- 1 Adler SP, Nigro G and Pereira L (2007) Recent advances in the prevention and treatment of congenital cytomegalovirus infections. *Semin Perinatol* **31**, 10–18.

- 2 Sissons JG and Carmichael AJ (2002) Clinical aspects and management of cytomegalovirus infection. *J Infect* **44**, 78–83.
- 3 Dollard SC, Grosse SD and Ross DS (2007) New estimates of the prevalence of neurological and sensory sequelae and mortality associated with congenital cytomegalovirus infection. *Rev Med Virol* **17**, 355–363.
- 4 Britt W (2008) Manifestations of human cytomegalovirus infection: proposed mechanisms of acute and chronic disease. *Curr Top Microbiol Immunol* **325**, 417–470.
- 5 Biron KK (2006) Antiviral drugs for cytomegalovirus diseases. *Antiviral Res* **71**, 154–163.
- 6 Freitas VR, Fraser-Smith EB and Matthews TR (1989) Increased efficacy of ganciclovir in combination with foscarnet against cytomegalovirus and herpes simplex virus type 2 *in vitro* and *in vivo*. *Antiviral Res* **12**, 205–212.
- 7 Noble S and Faulds D (1998) Ganciclovir. An update of its use in the prevention of cytomegalovirus infection and disease in transplant recipients. *Drugs* **56**, 115–146.
- 8 Deray G, Martinez F, Katlama C, Levaltier B, Beaufile H, Danis M, Rozenheim M, Baumelou A, Dohin E and Gentilini M (1989) Foscarnet nephrotoxicity: mechanism, incidence and prevention. *Am J Nephrol* **9**, 316–321.
- 9 Ho ES, Lin DC, Mendel DB and Cihlar T (2000) Cytotoxicity of antiviral nucleotides adefovir and cidofovir is induced by the expression of human renal organic anion transporter 1. *J Am Soc Nephrol* **11**, 383–393.
- 10 Akuzawa K, Yamada R, Li Z, Li Y, Sadanari H, Matsubara K, Watanabe K, Koketsu M, Tuchida Y and Murayama T (2011) Inhibitory effects of triclin derivative from *Sasa albo-marginata* on replication of human cytomegalovirus. *Antiviral Res* **91**, 296–303.
- 11 Yazawa K, Kurokawa M, Obuchi M, Li Y, Yamada R, Sadanari H, Matsubara K, Watanabe K, Koketsu M, Tuchida Y *et al.* (2011) Anti-influenza virus activity of triclin, 4',5,7-trihydroxy-3',5'-dimethoxyflavone. *Antivir Chem Chemother* **22**, 1–11.
- 12 Ninomiya M, Tanaka K, Tsuchida Y, Muto Y, Koketsu M and Watanabe K (2011) Increased bioavailability of triclin-amino acid derivatives via a prodrug approach. *J Med Chem* **54**, 1529–1536.
- 13 Murayama T, Li Y, Takahashi T, Yamada R, Matsubara K, Tuchida Y, Li Z and Sadanari H (2012) Anti-cytomegalovirus effects of triclin are dependent on CXCL11. *Microbes Infect* **14**, 1086–1092.
- 14 Akai Y, Sadanari H, Takemoto M, Uchide N, Daikoku T, Mukaida N and Murayama T (2017) Inhibition of human cytomegalovirus replication by triclin is associated with depressed CCL2 expression. *Antiviral Res* **148**, 15–19.
- 15 Kapasi AJ, Clark CL, Tran K and Spector DH (2009) Recruitment of cdk9 to the immediate-early viral transcriptosomes during human cytomegalovirus infection requires efficient binding to cyclin T1, a threshold level of IE2 86, and active transcription. *J Virol* **83**, 5904–5917.
- 16 Van Duyne R, Guendel I, Jaworski E, Sampey G, Klase Z, Chen H, Zeng C, Kovalsky D, El Kouni MH, Lepene B *et al.* (2013) Effect of mimetic CDK9 inhibitors on HIV-1-activated transcription. *J Mol Biol* **425**, 812–829.
- 17 Yamamoto M, Onogi H, Kii I, Yoshida S, Iida K, Sakai H, Abe M, Tsubota T, Ito N, Hosoya T *et al.* (2014) CDK9 inhibitor FIT-039 prevents replication of multiple DNA viruses. *J Clin Invest* **124**, 3479–3488.
- 18 Levin NMB, Pintro VO, de Ávila MB, de Mattos BB and de Azevedo WF Jr (2017) Understanding the structural basis for inhibition of cyclin-dependent kinases. New pieces in the molecular puzzle. *Curr Drug Targets* **18**, 1104–1111.
- 19 Meinhardt A, Kamenski T, Hoepfner S, Baumli S and Cramer P (2005) A structural perspective of CTD function. *Genes Dev* **19**, 1401–1415.
- 20 Glover-Cutter K, Larochelle S, Erickson B, Zhang C, Shokat K, Fisher RP and Bentley DL (2009) TFIIF-associated Cdk7 kinase functions in phosphorylation of C-terminal domain Ser7 residues, promoter-proximal pausing, and termination by RNA polymerase II. *Mol Cell Biol* **29**, 5455–5464.
- 21 De Azevedo WF, Mueller-Dieckmann HJ, Schulze-Gahmen U, Worland PJ, Sausville E and Kim SH (1996) Structural basis for specificity and potency of a flavonoid inhibitor of human CDK2, a cell cycle kinase. *Proc Natl Acad Sci USA* **93**, 2735–2740.
- 22 Thomas JP, Tutsch KD, Cleary JF, Bailey HH, Arzooonian R, Alberti D, Simon K, Feierabend C, Binger K, Marnocha R *et al.* (2002) Phase I clinical and pharmacokinetic trial of the cyclin-dependent kinase inhibitor flavopiridol. *Cancer Chemother Pharmacol* **50**, 465–472.
- 23 Chao S-H, Fujinaga K, Marion JE, Taube R, Sausville EA, Senderowicz AM, Peterlin BM and Price DH (2000) Flavopiridol inhibits P-TEFb and blocks HIV-1 replication. *J Biol Chem* **275**, 28345–28348.
- 24 Baumli S, Lolli G, Lowe ED, Troiani S, Rusconi L, Bullock AN, Debreczeni JÉ, Knapp S and Johnson LN (2008) The structure of P-TEFb (CDK9/cyclin T1), its complex with flavopiridol and regulation by phosphorylation. *EMBO J* **27**, 1907–1918.
- 25 Karaboga D and Basturk B (2007) A powerful and efficient algorithm for numerical function optimization: artificial bee colony (ABC) algorithm. *J Glob Optim* **39**, 459–471.
- 26 Das S, Biswas S and Kundu S (2013) Synergizing fitness learning with proximity-based food source selection in artificial bee colony algorithm for numerical optimization. *Appl Soft Comput* **13**, 4676–4694.

- 27 Uehara S, Fujimoto KJ and Tanaka S (2015) Protein–ligand docking using fitness learning-based artificial bee colony with proximity stimuli. *Phys Chem Chem Phys* **17**, 16412–16417.
- 28 Heberlé G and de Azevedo WF Jr (2011) Bio-inspired algorithms applied to molecular docking simulations. *Curr Med Chem* **18**, 1339–1352.
- 29 Lee C, Yang W-T and Parr RG (1988) Development of the Colle-Salvetti correlation-energy formula into a functional of the electron density. *Phys Rev B* **37**, 785–789.
- 30 Besler BH, Merz KM Jr and Kollman PA (1990) Atomic charges derived from semiempirical methods. *J Comput Chem* **11**, 431–439.
- 31 Frisch MJ, Trucks GW, Schlegel HB, Scuseria GE, Robb MA, Cheeseman JR, Scalmani G, Barone V, Mennucci B, Petersson GA *et al.* Gaussian09, Revision A.02. Gaussian, Inc., Wallingford, CT, 2009.
- 32 Huey R, Morris GM, Olson AJ and Goodsell DS (2007) A semiempirical free energy force field with charge-based desolvation. *J Comput Chem* **28**, 1145–1152.
- 33 Bodaghi B, Jones TR, Zipeto D, Vita C, Sun L, Laurent L, Arenzana-Seisdedos F, Virelizier JL and Michelson S (1998) Chemokine sequestration by viral chemoreceptors as a novel viral escape strategy: withdrawal of chemokines from the environment of cytomegalovirus-infected cells. *J Exp Med* **188**, 855–866.
- 34 Furukawa T, Fioretti A and Plotkin S (1973) Growth characteristics of cytomegalovirus in human fibroblasts with demonstration of protein synthesis early in viral replication. *J Virol* **11**, 991–997.
- 35 Wentworth BB and French L (1970) Plaque assay of cytomegalovirus strains of human origin. *Proc Soc Exp Biol Med* **135**, 253–258.
- 36 Morales F and Giordano A (2016) Overview of CDK9 as a target in cancer research. *Cell Cycle* **15**, 519–527.
- 37 Sonawane YA, Taylor MA, Napoleon JV, Rana S, Contreras JI and Natarajan A (2016) Cyclin dependent kinase 9 inhibitors for cancer therapy. *J Med Chem* **59**, 8667–8684.
- 38 de Azevedo WF Jr, Canduri F and da Silveira NJF (2002) Structural basis for inhibition of cyclin-dependent kinase 9 by flavopiridol. *Biochem Biophys Res Commun* **293**, 566–571.
- 39 Byth KF, Thomas A, Hughes G, Forder C, McGregor A, Geh C, Oakes S, Green C, Walker M, Newcombe N *et al.* (2009) AZD5438, a potent oral inhibitor of cyclin-dependent kinases 1, 2, and 9, leads to pharmacodynamic changes and potent antitumor effects in human tumor xenografts. *Mol Cancer Ther* **8**, 1856–1866.
- 40 Plewczynski D, Łaźniewski M, Augustyniak R and Ginalski K (2011) Can we trust docking results? Evaluation of seven commonly used programs on PDB bind database *J Comput Chem* **32**, 742–755.
- 41 Sakai A, Watanabe K, Koketsu M, Akuzawa K, Yamada R, Li Z, Sadanari H, Matsubara K and Murayama T (2008) Anti-human cytomegalovirus activity of constituents from *Sasa albo-marginata* (Kumazasa in Japan). *Antivir Chem Chemother* **19**, 125–132.